PHYSICAL REVIEW D **92,** 045045 (2015)

Quantum synchrotron radiation in the case of a field with finite extension

Tobias N. Wistisen
CERN, Geneva, Switzerland
(Received 23 June 2015; published 31 August 2015)

The semiclassical operator method of Baier and Katkov allows one to obtain the spectrum of synchrotron radiation in a way similar to the classical derivation but which is fully valid also in the quantum case of very strong electromagnetic fields. In the usual calculation the extension of the field is taken to be infinite. In this paper we apply a numerical routine based on the semiclassical operator method to the case of a constant field but with a finite extension. For large extensions of the field one obtains the usual result of quantum synchrotron radiation, while in the limit of small extension of the field one obtains a spectrum resembling that of bremsstrahlung. We derive a formula for the radiation spectrum in this limit. In the transition toward shorter field extensions one finds that the power-spectrum increases for soft photons and slightly diminishes for harder photons. It is found that in the classical case the total power emitted decreases as the field extension decreases while in the quantum case the total power emitted is first increased and then decreases. Such an effect could be important for future e^+e^- colliders such as the ILC or CLIC where the dominant energy and luminosity loss is due to synchrotron radiation by an e^-/e^+ in the field of the opposing bunch, often termed "beamstrahlung." In this paper we also discuss how these effects, in the quantum case could be measured in an experiment using thin aligned single crystals and high energy electrons available at e.g. the CERN SPS North Area, and in the classical case could already be relevant at existing accelerators with conventional magnets providing the electromagnetic field.

DOI: 10.1103/PhysRevD.92.045045 PACS numbers: 03.65.Sq, 11.15.Kc, 41.60.Ap

I. INTRODUCTION

In the field of strong field QED, processes whose description defy the usual application of the perturbative expansion in orders of α are of major interest. Until recently only a handful of analytical solutions existed in this case, namely the case of a plane wave field and the constant crossed field, see e.g. [1]. Recently analytical solutions in strong fields for the cases of ultrashort laser pulses have been found [2,3]. In this paper we will likewise investigate radiation emission by electrons in a nontrivial field configuration.

The result of quantum synchrotron radiation was first derived by N. P. Klepikov [4] and has been studied by several notable physicists in the field of QED [5–7]. The semiclassical operator method of V. N. Baier and V. M. Katkov seen in e.g. [8,9] provides a powerful method for the calculation of such processes. In [10] it is discussed how this method can be rewritten in a form similar to the classical formula of radiation emission as seen in e.g. [11] which allows one to find the radiation emission spectrum in any electromagnetic field by numerical methods. As seen in e.g. [1,12] a more traditional approach to the problem consists of finding the exact wave function of the Dirac equation where the constant crossed field is included exactly [13], and then treating the radiation emission to first order in perturbation theory. If the field is no longer "simple" e.g. a constant crossed field, finding the exact wave function is not a trivial task. The semiclassical operator method is powerful here, in the sense that finding this wave function is unnecessary—the classical motion in the field is sufficient. In Sec. II we will briefly introduce the theoretical formalism forming the basis of the numerical routine (see also [10] for this). In Sec. III we discuss the usual result of quantum synchrotron radiation and when the field should be considered "short." In Sec. IV we discuss the results of the numerical solution in the limit of short and "long" extensions of the field, as well as what happens in the intermediate region. In Sec. V we derive an analytical formula for the radiation spectrum in the limit of a short extension of the field. In Sec. VI we discuss the relevance of the obtained results in future colliders and how one could study these phenomena experimentally.

We use units where $\hbar = c = 1$ and $e^2 = \alpha \simeq \frac{1}{137}$, unless otherwise stated. For 4-vectors we employ the $(+,-,-,-)$ metric and the dot product of two 4-vectors is defined as the contraction i.e. $ab = a^\mu b_\mu$.

II. THEORETICAL FORMALISM

It is well known that some radiation phenomena are well described using classical electrodynamics such

as synchrotron and undulator/wiggler radiation, while others, such as radiation from atomic transitions, are not. Bohr's correspondence principle dictates that in the limit of large quantum numbers, quantum theory must reduce to that of classical physics. Atomic states have relatively low quantum numbers, compared to for instance a high energy electron in a magnetic field of typical laboratory field strengths. The case of synchrotron radiation, where an electron moves in a magnetic field, can be solved quantum mechanically giving the well-known Landau levels and the level spacing ω_L given by the cyclotron frequency, the classical frequency of revolution. The quantum number is therefore given by the particle energy ε and is $\frac{\varepsilon}{\omega_L} = \frac{\gamma^2 B_0}{B}$ where γ is the relativistic gamma factor and $B_0 = \frac{m^2}{e} \simeq 4.4 \times 10^9$ T is the Schwinger critical magnetic field. This means that as the particle energy increases, the motion becomes increasingly classical, and a trajectory as opposed to a wave function is an accurate description of the motion. However, the radiation process itself can be quantum mechanical, even if the motion is classical. Quantum effects become important in the radiation process when the emitted photon energy can no longer be neglected in comparison to the particle energy, meaning a condition for a classical treatment is $\omega \ll \varepsilon$, or in other words that the particle recoil due to radiation emission is negligible. Analytical applications of the semiclassical operator method show that this is equivalent with $\chi \ll 1$, i.e. χ is the relevant parameter when deciding whether quantum theory is necessary, see [9] for a more thorough discussion of this subject. Here we defined

$$\chi = \frac{e\sqrt{\langle (F_{\mu\nu} p^\nu)^2 \rangle}}{m^3}, \tag{1}$$

where $F_{\mu\nu}$ is the electromagnetic field tensor, p^ν the electron 4-momentum and m the electron mass. In the case of a constant magnetic field this becomes

$$\chi = \gamma \frac{B}{B_0}, \tag{2}$$

where γ is the Lorentz factor of the incoming particle and B the magnetic field strength.

The essence of the semiclassical operator method [9,14] is the neglect of quantum effects in the motion of the energetic particle, while treating the radiation emission quantum mechanically. This powerful result means that the classical trajectory completely determines the radiation emitted, also in the quantum regime.

In strong field QED, in addition to the parameter χ, often called the quantum nonlinearity parameter, one also introduces the classical nonlinearity parameter which in the case of a plane wave field is

$$\xi = \frac{eE_{\text{r.m.s.}}}{m\omega}, \tag{3}$$

where $E_{\text{r.m.s.}}$ is the r.m.s. electric field strength and ω the angular frequency of the plane wave field. In the case of a plane wave field the two nonlinearity parameters χ and ξ can be varied individually to give a variety of cases. In the case of a plane wave field, edges are found in the emission spectrum corresponding to absorption of s number of photons given by the formula

$$\omega_s = \frac{4s\omega\varepsilon^2}{\bar{m}^2 + 4s\omega\varepsilon + \varepsilon^2\theta^2}, \tag{4}$$

where $\bar{m}^2 = m^2(1+\xi^2)$ and θ the angle of the emitted photon. Some controversy surrounds the effective mass $\bar{m}$ [2,15,16] and it has not yet been demonstrated experimentally. As ξ increases from 0 the increased effective mass moves the kinematic edge found in the emission spectrum toward a lower photon energy as seen from Eq. (4) (the edge corresponds to $\theta = 0$). In addition the higher harmonics ($s > 1$) become dominant. The case of the constant crossed field can be seen to correspond with letting $\omega \to 0$ in Eq. (3) or $\bar{m} \to \infty$. In this case the spectrum will consist of a sum of many harmonics which have become very downshifted due to the increased effective mass—the sum of which add up to the well-known constant crossed field result to be discussed later. The shape of the spectrum in the case of the constant crossed field of infinite extension is thus determined only by the single parameter χ.

We employ a formula seen in [17], derived and discussed in detail in [10], of the radiation emission similar to the classical result [11]. In this approach the electromagnetic coupling of the electron to the incoming electromagnetic field is treated exactly i.e. without the use of perturbation theory while the coupling to the outgoing electromagnetic field leading to emission is treated to first order in perturbation theory.

As seen in [10,17] the energy emitted differential in photon energy and solid angle, in the case of an initially unpolarized electron, and summing over final spins is given by

$$\frac{d^2 I}{d\omega d\Omega} = \frac{e^2}{4\pi^2}\left(\frac{\varepsilon'^2 + \varepsilon^2}{2\varepsilon^2}|\boldsymbol{I}|^2 + \frac{\omega^2 m^2}{2\varepsilon^4}|J|^2\right). \tag{5}$$

In [10] one also finds the contribution when the initial electron beam is polarized, which in the case of a constant field gives additional contributions when the beams are polarized transversely to the velocity. In a collider, however, the beams will be longitudinally polarized and these terms vanish. Thus we consider the case of an unpolarized beam. We have defined

$$\boldsymbol{I} = \int_{-\infty}^{\infty} \boldsymbol{f}(t,\boldsymbol{n}) e^{ik'x} dt, \tag{6}$$

$$J = \int_{-\infty}^{\infty} \frac{\boldsymbol{n}\cdot\dot{\boldsymbol{v}}}{(1-\boldsymbol{n}\cdot\boldsymbol{v})^2} e^{ik'x} dt, \tag{7}$$

where k is the photon 4-momentum, $x(t) = (t, \boldsymbol{x}(t))$, where $\boldsymbol{x}(t)$ is the solution of the relativistic equation of motion using the Lorentz force given by the background field, $k' = \frac{\varepsilon}{\varepsilon'} k$, $\varepsilon' = \varepsilon - \omega$ and $\boldsymbol{n}$ is a unit vector in the direction of $\boldsymbol{k}$. We will also use the notation $\omega' = \omega \frac{\varepsilon}{\varepsilon'}$. We have defined

$$\boldsymbol{f}(t,\boldsymbol{n}) = \frac{\boldsymbol{n}\times[(\boldsymbol{n}-\boldsymbol{v})\times\dot{\boldsymbol{v}}]}{(1-\boldsymbol{v}\cdot\boldsymbol{n})^2}, \tag{8}$$

where $\boldsymbol{v} = \dot{\boldsymbol{x}}$ is the velocity and $\dot{\boldsymbol{v}}$ the acceleration. In addition we have the useful relations

$$\begin{aligned}\int_{-\infty}^{\infty} &(\boldsymbol{n}-\boldsymbol{v}) e^{ik'x} dt \\ &= \int_{-\infty}^{\infty} \boldsymbol{n}\times(\boldsymbol{n}\times\boldsymbol{v}) e^{ik'x} dt \\ &= -\frac{1}{i\omega'} \int_{-\infty}^{\infty} \boldsymbol{f}(t,\boldsymbol{n}) e^{ik'x} dt = \frac{i}{\omega'} \boldsymbol{I},\end{aligned} \tag{9}$$

and

$$\begin{aligned}\int_{-\infty}^{\infty} e^{ik'x} dt &= \int_{-\infty}^{\infty} \boldsymbol{n}\cdot\boldsymbol{v} e^{ik'x} dt \\ &= \int_{-\infty}^{\infty} \frac{\boldsymbol{n}\cdot\boldsymbol{v}}{1-\boldsymbol{n}\cdot\boldsymbol{v}} \frac{1}{i\omega'} \frac{d}{dt} (e^{ik'x}) dt \\ &= -\frac{1}{i\omega'} \int_{-\infty}^{\infty} \frac{\boldsymbol{n}\cdot\dot{\boldsymbol{v}}}{(1-\boldsymbol{n}\cdot\boldsymbol{v})^2} e^{ik'x} dt = \frac{i}{\omega'} J.\end{aligned} \tag{10}$$

We define the "phase" as the function.

$$\phi = k'x = \omega'(t - \boldsymbol{n}\cdot\boldsymbol{x}(t)). \tag{11}$$

We remind the reader that the classical result for the radiation emission instead of Eq. (5) is given by

$$\frac{d^2 I}{d\omega d\Omega} = \frac{e^2}{4\pi^2} \left| \int_{-\infty}^{\infty} \boldsymbol{f}(t,\boldsymbol{n}) e^{ikx} dt \right|^2. \tag{12}$$

The initial direction of motion is chosen along the z-axis and we therefore define $\delta z = z - v_0 t$ where $v_0 \simeq 1 - \frac{1}{2\gamma^2}$ and θ_x, θ_y are the small transverse components of $\boldsymbol{n}$ such that $\boldsymbol{n} = (\theta_x, \theta_y, 1 - \frac{\theta^2}{2})$ and $\theta^2 = \theta_x^2 + \theta_y^2$. We then expand Eq. (8) to leading order in the small quantities v_x, v_y, θ_x, θ_y and $1/\gamma$ to obtain

$$\begin{aligned} f_x = g\Big\{ &\theta_y[(\theta_x - v_x)\dot{v}_y - (\theta_y - v_y)\dot{v}_x] \\ &- \left(\frac{1}{2\gamma^2} - \frac{\theta^2}{2} - \delta v_z\right)\dot{v}_x + (\theta_x - v_x)\delta\dot{v}_z \Big\}, \end{aligned} \tag{13}$$

$$\begin{aligned} f_y = g\Big\{ &(\theta_y - v_y)\delta\dot{v}_z - \left(\frac{1}{2\gamma^2} - \frac{\theta^2}{2} - \delta v_z\right)\dot{v}_y \\ &- \theta_x[(\theta_x - v_x)\dot{v}_y - (\theta_y - v_y)\dot{v}_x] \Big\}, \end{aligned} \tag{14}$$

$$\begin{aligned} f_z = g\Big\{ &\theta_x\left[\left(\frac{1}{2\gamma^2} - \frac{\theta^2}{2} - \delta v_z\right)\dot{v}_x - (\theta_x - v_x)\delta\dot{v}_z\right] \\ &- \theta_y\left[(\theta_y - v_y)\delta\dot{v}_z - \left(\frac{1}{2\gamma^2} - \frac{\theta^2}{2} - \delta v_z\right)\dot{v}_y\right] \Big\}, \end{aligned} \tag{15}$$

and

$$\boldsymbol{n}\cdot\dot{\boldsymbol{v}} = g\{\boldsymbol{n}_\perp\cdot\dot{\boldsymbol{v}}_\perp + \delta\dot{v}_z\} \tag{16}$$

where we have defined $\boldsymbol{n}_\perp = (\theta_x, \theta_y)$, $\boldsymbol{v}_\perp = (v_x, v_y)$ and

$$g = \left(\frac{1}{2\gamma^2} + \frac{\theta^2}{2} - \delta v_z - \boldsymbol{n}_\perp\cdot\boldsymbol{v}_\perp\right)^{-2}. \tag{17}$$

Similarly the exponential phase becomes

$$k'x = \frac{\varepsilon}{\varepsilon'}\omega\left(\left(\frac{1}{2\gamma^2} + \frac{\theta^2}{2}\right)t - \delta z(t) - \boldsymbol{n}_\perp\cdot\boldsymbol{x}_\perp(t)\right). \tag{18}$$

f_z is suppressed by $\frac{1}{\gamma}$ compared to f_x and f_y, and can thus be neglected.

III. SYNCHROTRON RADIATION

Because of the similarity of Eq. (5) with the classical result, one can follow a calculation completely analogous to the one found in [11] to obtain the distribution of synchrotron radiation, but valid also in the quantum case. Synchrotron radiation is obtained by using Eq. (5) and the motion as described by

$$v_x = v\sin\left(\frac{vt}{R}\right), \tag{19}$$

$$v_y = 0, \tag{20}$$

$$v_z = v\cos\left(\frac{vt}{R}\right), \tag{21}$$

where $R = \frac{p}{eB}$ is the radius of curvature, v the velocity and t the time coordinate. To obtain $\boldsymbol{I}$ we calculate $\int(\boldsymbol{n}-\boldsymbol{v})e^{ik'x}dt$, see Eq. (9). Due to the symmetry of the

motion it is known *a priori* that the radiation spectrum must be independent of θ_x and thus we can choose our coordinate system such that $\theta_x = 0$ as done in [11]. This means $\theta = \theta_y$. Then we can calculate the phase using Eq. (18).

$$k'x = \omega'\left(\left(\frac{1}{2\gamma^2} + \frac{\theta^2}{2}\right)t + \frac{t^3}{6R^2}\right). \tag{22}$$

We then find

$$\begin{aligned}\int_{-\infty}^{\infty} (\boldsymbol{n}-\boldsymbol{v})_x e^{ik'x} dt &= \int_{-\infty}^{\infty} -v \sin\left(\frac{vt}{R}\right) e^{ik'x} dt \\ &= -\frac{v^2}{R}\int te^{ik'x} dt \\ &= -\frac{1}{R}\int_{-\infty}^{\infty} te^{i\frac{\omega' t}{2}(\theta^2 + \frac{1}{\gamma^2} + \frac{v^2 t^2}{3R^2})} dt.\end{aligned} \tag{23}$$

Changing variable to $x = \frac{t}{R\sqrt{\frac{1}{\gamma^2}+\theta^2}}$ and introducing $\xi = \frac{\omega' R}{3}(\frac{1}{\gamma^2} + \theta^2)^{\frac{3}{2}}$ this becomes

$$\begin{aligned}&\int_{-\infty}^{\infty} (\boldsymbol{n}-\boldsymbol{v})_x e^{ik'x} dt \\ &= -R\left(\frac{1}{\gamma^2} + \theta^2\right)\int_{-\infty}^{\infty} x \exp\left(i\frac{3}{2}\xi\left(x + \frac{x^3}{3}\right)\right) dx \\ &= -R\left(\frac{1}{\gamma^2} + \theta^2\right)\frac{2i}{\sqrt{3}} K_{2/3}(\xi)\end{aligned} \tag{24}$$

where K_α denotes the modified Bessel function of the second kind of order α. Similarly we calculate

$$\begin{aligned}&\int_{-\infty}^{\infty} (\boldsymbol{n}-\boldsymbol{v})_y e^{ik'x} dt \\ &= \theta\int_{-\infty}^{\infty} e^{i\frac{\omega' t}{2}(\theta^2 + \frac{1}{\gamma^2} + \frac{v^2 t^2}{3R^2})} dt \\ &= R\theta\left(\frac{1}{\gamma^2} + \theta^2\right)^{\frac{1}{2}}\int_{-\infty}^{\infty} \exp\left(i\frac{3}{2}\xi\left(x + \frac{x^3}{3}\right)\right) dx \\ &= R\theta\left(\frac{1}{\gamma^2} + \theta^2\right)^{\frac{1}{2}}\frac{2}{\sqrt{3}} K_{1/3}(\xi).\end{aligned} \tag{25}$$

To calculate J we need to calculate [see Eq. (10)]

$$\begin{aligned}\int_{-\infty}^{\infty} e^{ik'x} dt &= \int_{-\infty}^{\infty} e^{i\frac{\omega' t}{2}(\theta^2 + \frac{1}{\gamma^2} + \frac{v^2 t^2}{3R^2})} dt \\ &= R\left(\frac{1}{\gamma^2} + \theta^2\right)^{\frac{1}{2}}\frac{2}{\sqrt{3}} K_{1/3}(\xi).\end{aligned} \tag{26}$$

We therefore obtain

$$\begin{aligned}|\boldsymbol{I}|^2 &= \omega'^2\left(R^2\left(\frac{1}{\gamma^2} + \theta^2\right)^2\frac{4}{3}K_{2/3}^2(\xi) \right. \\ &\quad \left. + R^2\theta^2\left(\frac{1}{\gamma^2} + \theta^2\right)\frac{4}{3}K_{1/3}^2(\xi)\right) \\ &= \frac{\varepsilon^2}{\varepsilon'^2}(\omega R)^2\frac{4}{3}\left(\frac{1}{\gamma^2} + \theta^2\right)^2\left(K_{2/3}^2(\xi) + \frac{\theta^2}{\frac{1}{\gamma^2} + \theta^2}K_{1/3}^2(\xi)\right)\end{aligned} \tag{27}$$

and

$$\begin{aligned}|J|^2 &= \omega'^2\left[R\left(\frac{1}{\gamma^2} + \theta^2\right)^{\frac{1}{2}}\frac{2}{\sqrt{3}}K_{1/3}(\xi)\right]^2 \\ &= \frac{\varepsilon^2}{\varepsilon'^2}(\omega R)^2\left(\frac{1}{\gamma^2} + \theta^2\right)\frac{4}{3}K_{1/3}^2(\xi).\end{aligned} \tag{28}$$

By using Eq. (5) we obtain the energy spectrum of synchrotron radiation as

$$\begin{aligned}\frac{d^2 I}{d\omega d\Omega} &= \frac{e^2}{3\pi^2}(\omega R)^2\left(\frac{\varepsilon'^2 + \varepsilon^2}{2\varepsilon'^2}\left(\frac{1}{\gamma^2} + \theta^2\right)^2\right. \\ &\quad \times\left(K_{2/3}^2(\xi) + \frac{\theta^2}{\frac{1}{\gamma^2} + \theta^2}K_{1/3}^2(\xi)\right) \\ &\quad \left. + \frac{\omega^2 m^2}{2(\varepsilon\varepsilon')^2}\left(\frac{1}{\gamma^2} + \theta^2\right)K_{1/3}^2(\xi)\right).\end{aligned} \tag{29}$$

By writing $d\Omega = d\theta_x d\theta_y$ and integrating over θ_x from 0 to 2π and dividing by the period $2\pi R$ the differential power spectrum is obtained as

$$\begin{aligned}\frac{dP}{d\omega d\theta} &= \frac{e^2}{3\pi^2 R}(\omega R)^2\left(\frac{\varepsilon'^2 + \varepsilon^2}{2\varepsilon'^2}\left(\frac{1}{\gamma^2} + \theta^2\right)^2\right. \\ &\quad \times\left(K_{2/3}^2(\xi) + \frac{\theta^2}{\frac{1}{\gamma^2} + \theta^2}K_{1/3}^2(\xi)\right) \\ &\quad \left. + \frac{\omega^2 m^2}{2(\varepsilon\varepsilon')^2}\left(\frac{1}{\gamma^2} + \theta^2\right)K_{1/3}^2(\xi)\right).\end{aligned} \tag{30}$$

This formula is valid in the quantum regime as well. Integrating Eq. (30) over θ yields the usual result of quantum synchrotron radiation given by [9]

$$\begin{aligned}\frac{dP}{d\omega} &= \frac{e^2 m^2}{\pi\sqrt{3}}\frac{u}{(1+u)^3}\frac{du}{d\omega} \\ &\quad \times\left(\frac{u^2}{1+u}K_{2/3}\left(\frac{2u}{3\chi}\right) + \int_{\frac{2u}{3\chi}}^{\infty} K_{5/3}(y) dy\right)\end{aligned} \tag{31}$$

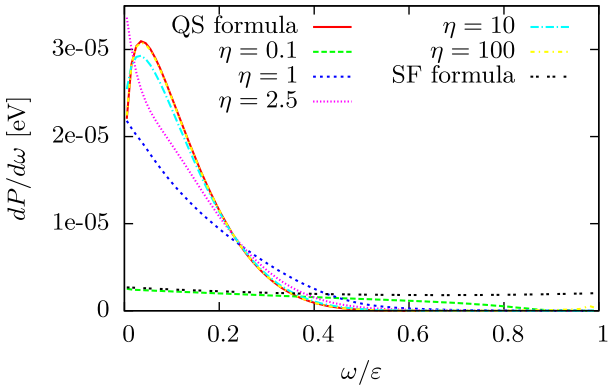

FIG. 1 (color online). A plot of the power spectra for the case $\chi = 0.1$, $\varepsilon = 1.5$ TeV and different values of η. QS formula is the formula of quantum synchrotron radiation seen in Eq. (31). SF formula is the short field formula of Eq. (51) for the case of $\eta = 0.1$.

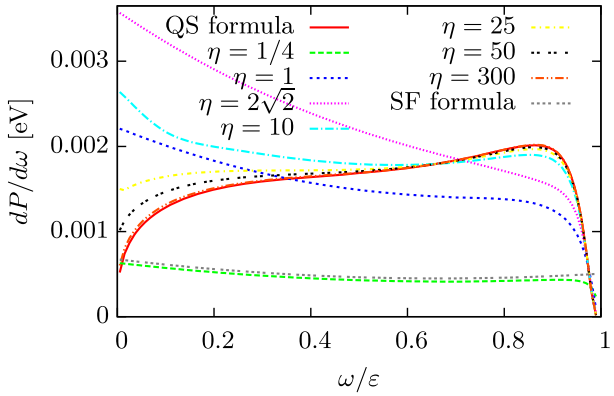

FIG. 2 (color online). A plot of the power spectra for the case $\chi = 10$, $\varepsilon = 1.5$ TeV and different values of η. QS formula is the formula of quantum synchrotron radiation seen in Eq. (31). SF formula is the short field formula of Eq. (51) for the case of $\eta = 1/4$.

where $u = \frac{\omega}{\varepsilon'}$. The integral of this spectrum with respect to the photon energy gives the total power which we denote P_0.

In this calculation a circular motion is assumed, lasting for times $-\infty < t < \infty$, as seen in Eqs. (19)–(21). In the case of a field with finite extension the motion can be characterized by that of Eqs. (19)–(21) when $-\frac{L}{2} < t < \frac{L}{2}$ and that the acceleration is 0 otherwise. For this reason we employ the formulas for $\boldsymbol{I}$ and J where the integrand is proportional to the acceleration such that the only difference in the numerical calculation is changing the integration limit. From Eq. (21) it can be shown that the condition $-\frac{L}{2} < t < \frac{L}{2}$ differs from the condition $-\frac{L}{2} < z < \frac{L}{2}$ only with a relative correction on the order of $\frac{1}{\gamma^2} + \frac{L^2}{R^2}$ which means that whether the field has a finite extension in time or in the z-direction is equivalent. The $\boldsymbol{I}$ term

$$\boldsymbol{I} = \int_{-\infty}^{\infty} \boldsymbol{f}(t, \boldsymbol{n}) e^{ik'x} dt, \tag{32}$$

becomes

$$\boldsymbol{I} = \int_{-\frac{L}{2}}^{\frac{L}{2}} \boldsymbol{f}(t, \boldsymbol{n}) e^{ik'x} dt, \tag{33}$$

and similarly for the J term. The angular distribution is then no longer known to be independent of θ_x and the integration limits means an analytical expression is no longer easily obtained. We can argue how small L should be for the difference between these two integrals to be significant. The formation length is the length over which the contributions from different parts of the trajectory add coherently and by setting $\phi \sim 1$ from Eq. (11). The corresponding length is given by

$$l_f = \frac{2\gamma^2}{\omega'} = \frac{2\gamma^2(\varepsilon - \omega)}{\omega\varepsilon}. \tag{34}$$

We can therefore recognize two cases. When $L \gg l_f$ we are in the usual regime of synchrotron radiation, while if $L \ll l_f$ the extension of the field can no longer be neglected. We therefore obtain the condition

$$\frac{\omega}{\varepsilon} \ll \frac{1}{1 + \frac{\varepsilon L}{2\gamma^2}}. \tag{35}$$

If we define $\eta = \gamma \frac{L}{R}$, meaning η is the deflection angle in units of $1/\gamma$, we can express the length as

$$L = \frac{\eta\gamma}{m\chi} \tag{36}$$

and so the condition becomes

$$\frac{\omega}{\varepsilon} \ll \frac{1}{1 + \frac{\eta}{2\chi}}. \tag{37}$$

We can thus consider the four cases

A. Case 1: $\eta \leq 1$ and $\eta \leq \chi$, the limit of short field extension

$\eta \leq 1$ is also commonly referred to as the dipole case and from Eq. (37) we see that the spectrum is modified for all photon energies up to the initial electron energy. In Sec. V we will derive an analytical result applicable in this case.

B. Case 2: $\eta \leq 1$ and $\eta \geq \chi$, the intermediate classical case

In this case we are still in the dipole case and the spectrum is modified when $\frac{\omega}{\varepsilon} \lesssim \frac{2\chi}{\eta}$ this means the spectrum is modified below frequencies of $\frac{1}{\eta}$ times the critical synchrotron frequency ω_c and is here given approximately by the dipole formula as shown in Sec. V. Since $\eta \leq 1$ this means the spectrum will always be modified at the critical synchrotron frequency or above. At photon energies above

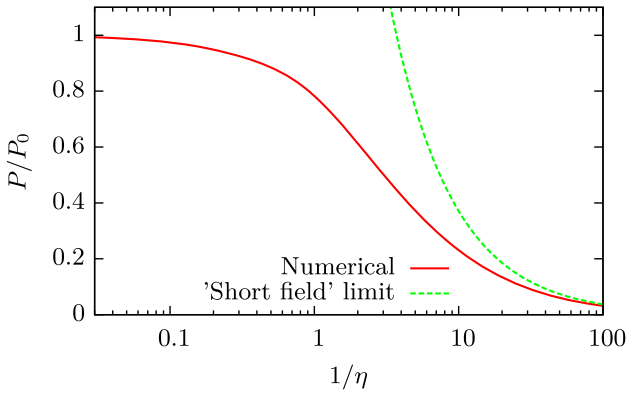

FIG. 3 (color online). A plot of the total power emitted in units of P_0 as function of $1/\eta$. In this case $\chi = 0.1$. The red curve is obtained by the numerical procedure described in the text and the green dashed curve is a plot of Eq. (52).

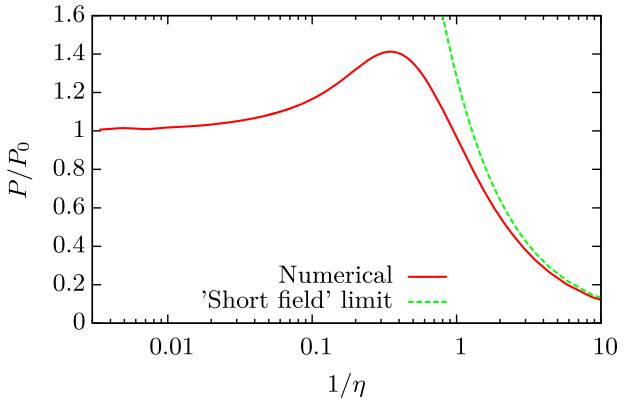

FIG. 4 (color online). A plot of the total power emitted in units of P_0 as function of $1/\eta$. In this case $\chi = 10$. The red curve is obtained by the numerical procedure described in the text and the green dashed curve is a plot of Eq. (52).

those corresponding to $\frac{\omega}{\varepsilon} \simeq \frac{2\chi}{\eta}$ the spectrum will transition to that of synchrotron radiation, which is vanishing above the critical frequency which means in effect that one has dipole spectrum up to this limit and then the spectrum will die out. An accurate spectrum can in this case only be obtained numerically.

C. Case 3: $\eta \geq 1$ and $\eta \leq \chi$, the intermediate quantum case

In this case the radiation spectrum is modified at roughly all photon energies and must also be calculated numerically.

D. Case 4: $\eta \geq 1$ and $\eta \geq \chi$, the limit of large field extension

In this case the spectrum is modified when $\frac{\omega}{\varepsilon} \lesssim \frac{2\chi}{\eta}$ which means the spectrum is modified below frequencies of $\frac{1}{\eta}$ times the critical synchrotron frequency ω_c. Since $\eta \geq 1$ this means the spectrum will always be modified only below the critical frequency, and thus for higher frequencies the spectrum is that of the usual synchrotron radiation. In the limit $\eta \gg \chi$ one obtains the usual result of Eq. (31).

From these 4 cases it is seen that whether one is in the classical case, $\chi \lesssim 1$ or the quantum case $\chi \gtrsim 1$ makes an important difference. In the classical case, as one transitions from larger to smaller values of η one goes from case 4 to case 2 and then to case 1. In the quantum case one goes from case 4 to case 3 and then to case 1. We can therefore define two characteristic lengths which determine the extension of the field where deviation from the usual synchrotron result is seen. In the classical case the transition from the usual result happens when one transitions from case 4 to case 2 i.e. $\eta \sim 1$, using Eq. (36) we thus define the characteristic classical length as

$$l_c = \frac{\gamma}{m\chi}. \tag{38}$$

In conventional units this does not contain $\hbar$ and is indeed a classical quantity. In the quantum case the transition takes place when between case 4 and 3 i.e. when $\eta \sim \chi$ and thus we define the characteristic quantum length of this problem as

$$l_q = \frac{\gamma}{m}, \tag{39}$$

which is a factor of γ times the reduced Compton wavelength—a quantum length scale. This case thus corresponds to the extension of the field in the rest frame of the electron being the reduced Compton wavelength.

IV. DISCUSSION OF NUMERICAL RESULTS

We employed a numerical method like the one used in [10]. In essence one performs a numerical calculation of the classical trajectory by solving the classical equations of motion in the given field. Here the field is a constant magnetic field in the region $-L/2 \leq z \leq L/2$ and no field otherwise. Then the integrals of Eqs. (6) and (7) are evaluated numerically by using the formulas Eqs. (13)–(18). This allows one to calculate the intensity distribution using Eq. (5) for a given photon energy ω and angle (θ_x, θ_y). Therefore for each photon energy these integrals must be calculated on an angular grid, and then integrated numerically over this grid to obtain the intensity distribution in photon energy $dI/d\omega$. This grid should be chosen large enough such that essentially all radiation falls within this grid. In Eq. (30) the variable of the Bessel function is $\xi = \frac{\omega' R}{3}(\frac{1}{\gamma^2} + \theta^2)^{\frac{3}{2}}$, and for large arguments the Bessel function decreases rapidly, thus the typical angle of the radiation is $\theta \lesssim (\frac{3}{\omega' R})^{\frac{1}{3}}$. If the deflection is along x as in Eq. (19) one can use the total deflection angle in x as a guide for the grid size in the x-direction and $\theta_y \lesssim (\frac{3}{\omega' R})^{\frac{1}{3}}$ for

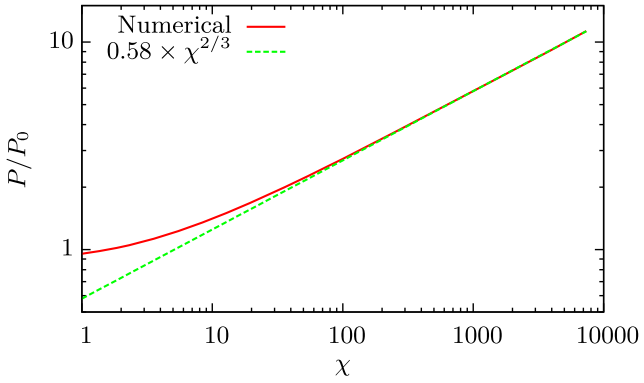

FIG. 5 (color online). A plot of the numerical values obtained for the power in the case of $\eta = 2\sqrt{2}$ where the power is at a maximum as function of χ and a plot of an analytical fit valid for large values of χ.

the y-direction. By plotting the angular distributions one can determine if a slightly larger grid is necessary.

In Figs. 1 and 2 plots of the power spectra calculated using this numerical procedure are shown for $\chi = 0.1$ and $\chi = 10$ for various values of η. In addition we have plotted the usual result of Eq. (31) where the field has infinite extension. For large values of η it is seen that the numerical result approaches this spectrum as is expected from the discussion in Sec. III D. As η becomes smaller i.e. the field extension L becomes smaller, the power spectrum becomes modified at the low end of the spectrum. Since the formation length becomes longer for low photon energies this effect can be understood in the sense that these will be more susceptible to the finite extension of the field. In the case of $\chi = 0.1$ seen in Fig. 1, as η becomes close to and below 1 a transition is observed where the spectrum is radically different. For $\eta = 0.1$ we are at the border of transition from case 2 to case 1. For comparison we have plotted Eq. (51), which is seen to be in good agreement for the low end of the spectrum. For even smaller values of η this agreement extends to the harder photons as well. In the case of $\chi = 10$ as seen in Fig. 2 the spectrum is seen to be modified for larger values of η than the case of $\chi = 0.1$. This is due to the fact that in the quantum regime the first transition is instead from case 4 to case 3, meaning at $\eta \sim \chi = 10$. Here we have also plotted the result of Eq. (51) for comparison, which is seen to be in good agreement.

In these plots a remarkable overall decrease in the power spectrum is seen when $\eta \lesssim 1$. In Figs. 3 and 4 we have plotted the total power P as a function of $1/\eta$ for the case of $\chi = 0.1$ and $\chi = 10$, respectively. P_0 is the total power as obtained by Eq. (31). For small values of $1/\eta$ the spectrum approaches that of Eq. (31), and therefore the total power approaches P_0. The difference between the classical and quantum case is clear in these two figures. In the classical case the intermediate regime of case 2 for $0.1 \leq \eta \leq 1$ shows a decrease in the total power emitted while the case of the intermediate quantum regime of case 3 shows an increase in the total power emitted. This maximum in the emitted power is found to be at $\eta = 2\sqrt{2}$ independently of χ for large values of χ. In Fig. 5 we show how this maximum emitted power scales with the value of χ. It is found that the numerical calculation agrees very well with the expression

$$\frac{P}{P_0} = 0.58\chi^{\frac{2}{3}} \tag{40}$$

for large values of χ.

V. THE SPECTRUM IN THE LIMIT OF A SHORT EXTENSION OF THE FIELD

In Sec. III A and Sec. III B we found that for all photon energies where there should be radiation, the formation length is much larger than the extension of the field, and thus the variation of the phase of Eq. (22) was negligible. Thus we can approximate

$$\boldsymbol{I} = \int_{-\frac{L}{2}}^{\frac{L}{2}} \boldsymbol{f}(t,\boldsymbol{n}) e^{ik'x} dt \simeq \int_{-\frac{L}{2}}^{\frac{L}{2}} \boldsymbol{f}(t,\boldsymbol{n}) dt.$$

We take the force to act in the x direction and thus only keep terms proportional to $\dot{v}_x$ in Eqs. (13) and (14). In these terms only the y-component of the velocity enters which is 0 and so we obtain

$$I_x = -g_0|\Delta\boldsymbol{v}|\left\{\theta_y^2 + \left(\frac{1}{2\gamma^2} - \frac{\theta^2}{2}\right)\right\}, \tag{41}$$

$$I_y = g_0|\Delta\boldsymbol{v}|\theta_x\theta_y, \tag{42}$$

where we have only kept the first order in the transverse velocity change $|\Delta\boldsymbol{v}|$ and

$$g_0 = \left(\frac{1}{2\gamma^2} + \frac{\theta^2}{2}\right)^{-2}.$$

For the J term we thus obtain

$$J = \int \frac{\boldsymbol{n}\cdot\dot{\boldsymbol{v}}}{(1-\boldsymbol{n}\cdot\boldsymbol{v})^2} e^{ik'x} dt \simeq g_0\theta_x|\Delta\boldsymbol{v}|.$$

Then we obtain

$$|\boldsymbol{I}|^2 = |\Delta\boldsymbol{v}|^2 g_0^2 \times \left(\theta_y^4 + \frac{1}{4\gamma^4} + \frac{\theta^4}{4} - \frac{\theta^2}{2\gamma^2} + \theta_y^2\left(\frac{1}{\gamma^2} - \theta^2\right) + \theta_x^2\theta_y^2\right).$$

Performing the integration over φ we obtain

$$\int |\boldsymbol{I}|^2 d\varphi = |\Delta\boldsymbol{v}|^2 g_0^2 \frac{\pi}{2}\frac{1}{\gamma^4}(1+\nu^4) \tag{43}$$

where $\nu = \gamma\theta$. Inserting g_0 this becomes

$$\int |\boldsymbol{I}|^2 d\varphi = |\Delta \boldsymbol{v}|^2 \frac{8\pi\gamma^4}{(1+\nu^2)^4}(1+\nu^4) \tag{44}$$

carrying out the integration $\int \theta d\theta = \frac{1}{\gamma^2}\int \nu d\nu$ we obtain

$$\int |\boldsymbol{I}|^2 d\Omega = \frac{8\pi}{3}\gamma^2 |\Delta \boldsymbol{v}|^2 \tag{45}$$

for the J term we obtain

$$|J|^2 = \frac{16\gamma^8}{(1+\nu^2)^4}\theta_x^2 |\Delta \boldsymbol{v}|^2 \tag{46}$$

integrating over φ we obtain

$$\int |J|^2 d\varphi = \frac{16\gamma^8}{(1+\nu^2)^4}\pi\theta^2 |\Delta \boldsymbol{v}|^2 \tag{47}$$

and integrating over $\theta d\theta$ we obtain

$$\int |J|^2 d\Omega = \frac{4}{3}\pi\gamma^4 |\Delta \boldsymbol{v}|^2. \tag{48}$$

We can therefore write the emitted energy differential in photon energy and angle variable ν by using Eq. (5) as

$$\frac{d^2 I}{d\omega d\nu} = \frac{2\alpha}{\pi}\gamma^2 |\Delta \boldsymbol{v}|^2 \times \left(\frac{\varepsilon'^2 + \varepsilon^2}{2\varepsilon^2}\frac{\nu(1+\nu^4)}{(1+\nu^2)^4} + \frac{\omega^2}{\varepsilon^2}\frac{\nu^3}{(1+\nu^2)^4}\right). \tag{49}$$

Integrating over ν one obtains the emitted energy differential in photon energy

$$\frac{dI}{d\omega} = \frac{2\alpha}{3\pi}\gamma^2 |\Delta \boldsymbol{v}|^2 \left(1 - \frac{\omega}{\varepsilon} + \frac{3}{4}\frac{\omega^2}{\varepsilon^2}\right). \tag{50}$$

Equations (49) and (50) are general and reduce to the classical formulas as found in e.g. [11] in the limit of $\omega \ll \varepsilon$. Inserting $\Delta v = \frac{eBL}{\varepsilon}$ and dividing by the duration L one obtains the power spectrum differential in photon energy in the case of the short magnetic field as

$$\frac{dP}{d\omega} = \frac{2\alpha}{3\pi\gamma^2}\chi^2 m^2 L \left(1 - \frac{\omega}{\varepsilon} + \frac{3}{4}\frac{\omega^2}{\varepsilon^2}\right). \tag{51}$$

The shape of this spectrum is the same of that of Bethe-Heitler bremsstrahlung in matter and thus in this limit synchrotron radiation becomes bremsstrahlung-like. In addition the power is now proportional to the length L in contrast to the usual synchrotron radiation power which is independent of the duration. Integrating this, one obtains the total power P as

$$P = \frac{\alpha}{2\pi}\frac{\chi^2 m^4 L}{\varepsilon} = \frac{\alpha}{2\pi}\chi\eta m^2. \tag{52}$$

VI. DISCUSSION OF EXPERIMENTAL INVESTIGATION AND RELEVANCE IN FUTURE COLLIDERS

From Eq. (38) it is seen that if γ is large while χ is small, the length at which this effect becomes important can become long. Consider as an example a 1 GeV synchrotron producing visible light of photon energy $\omega = 1$ eV, thus $\chi \sim 10^{-9}$ and the characteristic classical length is $l_c \sim 75$ cm. Thus in the classical case this should be an easily measurable effect under the right circumstances. In the quantum case when χ approaches or becomes larger than 1 it becomes experimentally challenging. In this case the characteristic length of Eq. (39) can only be made large by increasing the particle energy. The highest experimentally accessible electron energies are around 285 GeV found in secondary beams at the SPS North Area of CERN. At this energy the characteristic quantum length is 0.2 μm. Single crystals of Silicon can be purchased with lengths down to 0.1 μm, and by aligning the incoming beam along the $\langle 110 \rangle$ axis one can obtain $\chi \sim 1$, meaning one is in the quantum regime. At large energies the constant field approximation becomes applicable for the case of channeling radiation in such a crystal, meaning the results presented in this paper are applicable in this case.

In future e^+/e^- colliders such as CLIC, designed for the maximum energy per beam of $\varepsilon = 1.5$ TeV one achieves a quantum nonlinearity parameter of $\chi \sim 10$ [18] and with the current design parameters one has a bunch length of $\sigma_z = 44$ μm. In this case $l_q = 1.1$ μm. Often bunch shapes are modeled by a Gaussian distribution and we have numerically calculated spectra in the case when the electron is subject to a Gaussian shaped field pulse of varying length to verify that the effects seen in this paper are not an artefact present only in the case of a constant field with a sharp cutoff. Here the same effects are seen when the typical length scale of the bunch σ_z becomes comparable to the formation length. See e.g. [19] for recent experimental investigations of the significance of the formation length in the case of bremsstrahlung. From Figs. 4 and 2 it is seen that in the case of CLIC the effect is small—on the order of 1%. However such design parameters could change during development and thus this effect should be kept in mind.

ACKNOWLEDGMENTS

The author would like to thank Daniel Schulte for discussions regarding the design and development of CLIC. In addition the author would like to thank Ulrik I. Uggerhøj and Allan H. Sørensen for reading the manuscript and providing insightful suggestions.

[1] V. Ritus, J. Sov. Laser Res. **6**, 497 (1985).
[2] F. Mackenroth and A. Di Piazza, Phys. Rev. A **83**, 032106 (2011).
[3] D. Seipt and B. Kämpfer, Phys. Rev. A **83**, 022101 (2011).
[4] N. Klepikov, Zhur. Eksptl.'i Teoret. Fiz. **26** (1954).
[5] J. Schwinger and W. yang Tsai, Ann. Phys. (N.Y.) **110**, 63 (1978).
[6] A. A. Sokolov and I. M. Ternov, Akademia Nauk SSSR, Moskovskoie Obshchestvo Ispytatelei prirody. Sektsia Fiziki. Sinkhrotron Radiation, Nauka Eds., Moscow, 1966 (Russian title: Sinkhrotronnoie izluchenie) **228**, 1 (1966).
[7] J. Schwinger, W. yang Tsai, and T. Erber, Ann. Phys. (N.Y.) **96**, 303 (1976).
[8] V. Baier and V. Katkov, Sov. Phys. JETP **28**, 807 (1969).
[9] V. Baier, V. Katkov, and V. Strakhovenko, *Electromagnetic Processes at High Energies in Oriented Single Crystals* (World Scientific, Singapore, 1998).
[10] T. N. Wistisen, Phys. Rev. D **90**, 125008 (2014).
[11] J. D. Jackson, *Classical Electrodynamics*, 3rd ed. (John Wiley & Sons, Inc., New York, 1991).
[12] H. R. Reiss, J. Math. Phys. **3**, 59 (1962).
[13] D. Volkov, Z. Phys **94**, 250 (1935).
[14] V. B. Beresteckij, E. M. Lifsic, and L. P. Pitaevskij, *Quantum Electrodynamics* (Butterworth-Heinemann, Oxford, 2008).
[15] J. P. Corson and J. Peatross, Phys. Rev. A **85**, 046101 (2012).
[16] H. R. Reiss, Phys. Rev. A **89**, 022116 (2014).
[17] A. Belkacem, N. Cue, and J. Kimball, Phys. Lett. A **111**, 86 (1985).
[18] J. Esberg, U. I. Uggerhøj, B. Dalena, and D. Schulte, Phys. Rev. ST Accel. Beams **17**, 051003 (2014).
[19] K. Andersen, S. Andersen, H. Knudsen, R. Mikkelsen, H. Thomsen, U. Uggerhøj, T. Wistisen, J. Esberg, P. Sona, A. Mangiarotti *et al.*, Phys. Lett. B **732**, 309 (2014).